PHYSICAL REVIEW B VOLUME 3, NUMBER 12 15 JUNE 1971

# Influence of Band Inversion upon the Electrical Properties of $Pb_{0.77}Sn_{0.23}Se$†*

J. R. Dixon and G. F. Hoff
*Naval Ordnance Laboratory, White Oak, Silver Spring, Maryland* 20910
*and University of Maryland, College Park, Maryland* 20740
(Received 15 June 1970)

It is shown that the band-inversion phenomenon proposed by Dimmock, Melngailis, and Strauss should influence the electrical properties of $Pb_{0.77}Sn_{0.23}Se$. On the basis of a simple model, it is demonstrated that this influence should be pronounced for materials of low carrier concentration. This expectation is confirmed by our experimental studies of the electrical resistivity and Hall coefficient as a function of temperature, carrier concentration, and carrier type. In addition, an analysis of the data indicates that the effective mass of free carriers changes considerably with temperature as a result of the small and widely varying band gaps involved in the inversion phenomenon. Finally, there is no definitive experimental evidence of the multiple-band effects which have been reported for other materials of this type.

## I. INTRODUCTION

Lead-tin-selenide ($Pb_{1-x}Sn_xSe$) alloys in the range $0 < x < 0.4$ are semiconductors with rocksalt structure.[1] For these and the $Pb_{1-x}Sn_xTe$ alloys, the width of the energy gap $E_{gap}$ is strongly dependent upon both the alloy fraction $x$ and the temperature $T$. By changing $x$ and $T$ appropriately, $E_{gap}$ can be varied over wide ranges, which include very small values.[1,2] The unusual variability of $E_{gap}$ is believed to be explainable in terms of the band-inversion model first proposed by Dimmock *et al.*[2] for $Pb_{1-x}Sn_xTe$ and supported by the experimental data of Strauss for $Pb_{1-x}Sn_xSe$.[1] According to this model, as the Pb-Sn ratio is changed the valence and conduction bands progressively approach each other, touch, and then invert their roles. For a certain composition range in each system, the bands can also be inverted by changing the temperature of a given alloy.

Most of the past research on $Pb_{1-x}Sn_xSe$ alloys has dealt with variable-frequency infrared lasers and detectors[3-7] and with crystal preparation.[1,7-9] Very little is known concerning their electrical properties. An objective of the work reported here was to study these properties as a function of carrier type and concentration, in the expectation that under certain conditions they would be influenced strongly by phenomena associated with band inversion. Evidence of such influence is provided by the work of Strauss[1] who reported unusual sign reversals in the Hall coefficients of various $Pb_{1-x}Sn_xSe$ alloys as the temperature was lowered from 300 to 77 °K. In addition, abrupt variations in the temperature dependence of the resistivity of both $Pb_{1-x}Sn_xTe$ and $Pb_{1-x}Sn_xSe$ of high carrier concentration have been correlated with band-inversion phenomena.[10-12] More recently, we have reported a preliminary study on $p$-type $Pb_{0.77}Sn_{0.23}Se$ of low carrier concentration in which it is shown that large variations in the temperature dependence of both the Hall coefficient and resistivity are associated with band inversion.[13] The research reported here is an extension of the latter work. The $Pb_{0.77}Sn_{0.23}Se$ alloy was selected for study because we believed that the phenomena mentioned above would be strongly manifested in this material at convenient temperatures.

Another equally important objective of our work was to obtain information concerning other features of the over-all valence-conduction-band structure. Although a considerable amount of experimental evidence exists which supports the reality of the band-inversion phenomenon in this material, there is very little experimental information concerning the significance of other possible complicating band features such as band distortions and multiple bands. In general, such features would be expected to influence the electrical properties in distinctive and observable ways. We believed that our measurements would yield useful information concerning these topics.

## II. EXPERIMENTAL

The $Pb_{0.77}Sn_{0.23}Se$ crystals used in this study were prepared by the gradient-freeze technique. The starting alloy was obtained by melting the elements in a sealed quartz ampoule and quenching. The crystals were grown by transferring this alloy to a second ampoule with a conical tip, melting it in a vertical furnace with a temperature gradient, and freezing the melt from the bottom up at a rate of about 0.2 in./h. The freezing was accomplished by lowering the temperature uniformly at a rate of about 2 °C/h. The polycrystalline materials grown in this way had crystallite dimensions ranging from 1 to 5 mm. Metallurgical examination showed no evidence of metallic inclusions. The alloy fraction $x$ was determined by measuring the lattice constant $a_0$ using standard powder x-ray techniques

and by applying the relation[1,14]

$$a_0 = 6.127 - 0.12x \text{ Å}. \quad (1)$$

No significant variation in $x$ was found along the length of the ingots except very near the ends. The value of $x$ in the central uniform region was characteristically a few percent less than that of the starting alloy.

Hall samples were formed from the parent ingot using standard cutting and lapping techniques. They consisted of rectangular parallelepipeds approximately $1.2\times1.3\times5.0$ mm$^3$. Low-field Hall coefficients $R_H$ and resistivities $\rho$ were determined by the usual dc potentiometric methods. Extrinsic-carrier concentrations $N$ and Hall mobilities $\mu_H$ were obtained from these measurements by employing the relations

$$N = 1/e\left|R_H(4.2\,^\circ\text{K})\right| , \quad (2)$$

$$\mu_H(T) = R_H(T)/\rho(T) . \quad (3)$$

Various temperatures $T$ were achieved by placing the samples in an open liquid-helium Dewar and allowing the system to warm slowly to room temperature. The warming period was approximately 12 h. The temperature was monitored by a gold +3% iron vs copper thermocouple from 4.2 to 20 °K and by a copper vs constantan thermocouple from 20 to 300 °K.

Extrinsic-carrier concentrations were varied from the as-grown hole concentration of $P = 3.7\times10^{19}$ cm$^{-3}$ by various isothermal heat treatments. We believe that the extrinsic-carrier concentration for our crystals is due primarily to the presence of ionized lattice defects associated with deviations from stiochiometry[15] and that our heat treatments served to control these deviations.[8] A possible exception applies to sample A, as discussed in the next paragraph. Large hole concentrations were obtained by annealing samples at high temperatures in the presence of a Se-rich ingot of $Pb_{0.77}Sn_{0.23}Se$. The annealing period was followed by a rapid quench in water. Samples of large free-electron concentrations were obtained by the same method but with a Se-deficient ingot. Low carrier concentrations of both $n$ and $p$ type were obtained by anneals at relatively low temperatures with a Se-deficient ingot. The annealing temperatures, annealing times, and the resulting electrical properties are listed in Table I for all of our samples.

The $p$-type nature of sample A was unexpected because heat treatment in the presence of a Se-deficient ingot would normally be expected to yield $n$-type material. We have established on the basis of various experimental tests that the sample is homogeneous and that the result is reproducible. These findings suggest that impurities are playing a significant role as acceptor defects in sample A.

## III. MECHANISMS

In general, the Hall coefficient $R_H$ and electrical resistivity $\rho$ can be expressed functionally as

$$R_H = f(n,p,b,T,\gamma),$$
$$\rho = g(n,p,\mu_n,\mu_p,T,\delta). \quad (4)$$

In these relations, $n$ and $p$ are the free-electron and free-hole concentrations, respectively; $\mu_n$ and $\mu_p$ are the corresponding carrier mobilities; $b$ is the mobility ratio $\mu_n/\mu_p$; and $T$ is the sample temperature. The remaining symbols $\gamma$ and $\delta$ collectively represent the dependences of $R_H$ and $\rho$ upon details of the valence- and conduction-band shapes. They normally involve phenomena which are second order in nature, such as nonparabolicities and anisotropies of the bands. The variables appearing in Eq. (4) are generally not independent of one another, their interrelationships involving the nature of the band structure and carrier scattering mechanisms. The various explicit forms of Eq. (4) are well known and will not be discussed here. However, we do wish to point out some of the phe-

TABLE I. Results of isothermal annealing of $Pb_{0.77}Sn_{0.23}Se$.

| Sample[a] | Type | Extrinsic-carrier concentration (cm$^{-3}$) 4.2 °K | Hall mobility (cm$^2$/V sec) 4.2 °K | 300 °K | Annealing temperature (°C) | Companion[b] ingot | Annealing time |
|---|---|---|---|---|---|---|---|
| A | $p$ | $2.3\times10^{17}$ | 2 080 | 310 | 550 | Se deficient | 24 days |
| B | $p$ | $2.1\times10^{20}$ | 70 | 40 | 725 | Se rich | 1 week |
| C | $n$ | $1.1\times10^{18}$ | 28 100 | 1080 | 575 | Se deficient | 12 days |
| D | $n$ | $1.7\times10^{19}$ | 2 620 | 650 | 625 | Se deficient | 24 days |

[a]All samples had cross-sectional areas less than $1.2\times1.3$ mm$^2$.
[b]The companion ingot was a $Pb_{0.77}Sn_{0.23}Se$ alloy with either a deficiency or an excess of Se.

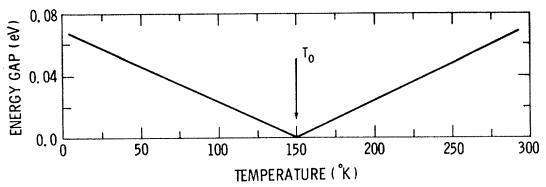


FIG. 1. Temperature dependence of the energy gap for the $Pb_{0.77}Sn_{0.23}Se$ alloy expected on the basis of experimental results and the band-inversion model.

nomena associated with band inversion which could influence $R_H$ and $\rho$.

One of these phenomena is directly connected with the unusual temperature dependence of $E_{gap}$ expected on the basis of the band-inversion model.[16] Such a dependence is illustrated in Fig. 1 for $Pb_{0.77}Sn_{0.23}Se$. This relationship was obtained by employing the experimental values for $E_{gap}$ which have been reported for various other alloy compositions,[1,4,5] along with linear interpolations based upon the band-inversion model. In deriving the relationship in this way, the expected decrease in the temperature coefficient of $E_{gap}$ below approximately[4] 30 °K has been neglected. However, we believe that this neglect does not have a significant bearing upon our analyses. The small gaps involved in the relationship of Fig. 1 suggest the possibility of thermally exciting enough carriers to influence the behavior of $R_H$ and $\rho$ at unusually low temperatures. We shall refer to all such situations as being intrinsiclike. Elementary reasoning leads to the expectation that intrinsiclike behavior should be strongly dependent upon the extrinsic-carrier concentration, being most pronounced for low concentrations. These assertions are supported by the illustrative calculations presented in Sec. IV.

There are several other phenomena associated with band inversion which could play significant roles in determining $R_H$ and $\rho$. For example, the small energy gaps involved could lead to valence-conduction-band distortions which would be large enough to influence the effective mass of the free carriers. In addition, multiple valence or conduction bands could lead to sizable carrier redistributions as the temperature is varied. The probable significance of these phenomena cannot be easily assessed theoretically. It is for this reason that a major objective of our work was to obtain experimental information concerning such phenomena.

## IV. ILLUSTRATIVE CALCULATIONS

In order to obtain a more quantitative description of the intrinsiclike behavior described in Sec. III, we have carried out calculations of $R_H$ and $\rho$ based upon an elementary band model undergoing inversion. We wish to emphasize that the model represents a simplification of the band structure one would expect under these conditions. Nevertheless, we feel that it is realistic enough to yield useful information regarding many of the major features in $R_H$ and $\rho$ arising from band inversion.

The model will be referred to as the constant-mass band-inversion model. It consists of parabolic valence and conduction bands which are mirror images of one another, each band being made up of four equivalent valleys. It is assumed that the energy gap separating these bands varies as indicated in Fig. 1. This is the only feature of band inversion which the model takes into account. We have not included the changes in symmetry of the valence and conduction bands which also accompany the inversion process. The reason for this omission is that such changes are expected to have only a relatively minor influence upon the electrical properties considered here.

Two of the important parameters involved in the calculations are the carrier effective mass $m^*$ and the electron-to-hole mobility ratio $b$. We have assumed that both of these parameters are independent of carrier concentration, temperature, and energy gap despite the fact that they are generally dependent upon these variables. These dependences are neglected in our model because their influences are expected to be second order in nature. The carrier effective mass of $0.1m_e$ employed in our calculations represents an upper limit of values expected for $Pb_{0.77}Sn_{0.23}Se$ over the range of temperature and carrier concentration considered here. Our estimate of this upper limit was based upon the effective masses reported for[17] PbSe and other $Pb_{1-x}Sn_xSe$ alloys.[5] Similarly, the mobility ratio of 2.0 which was used represents an upper limit of values to be expected on the basis of results reported for PbSe by Baryshev *et al.*[18]

The carrier concentrations $n$ and $p$ were determined as functions of temperature in a standard way.[19] This involved employing the Fermi-Dirac distribution function and the charge-neutrality relation

$$p = n \pm N, \tag{5}$$

in which $N$ is the concentration of extrinsic carriers. The plus and minus signs apply to $p$- and $n$-type materials, respectively. The extrinsic-carrier concentration is taken to be independent of temperature, an assumption based upon the fact that the donor and acceptor defects in closely related compounds have been found to be completely ionized at all temperatures.[17,20] The Hall coefficient corresponding to the calculated values of $n$ and $p$ was evaluated by applying the elementary two-carrier relation

$$R_H = (1/e)\,[p - b^2 n/(p + bn)^2]\ . \tag{6}$$

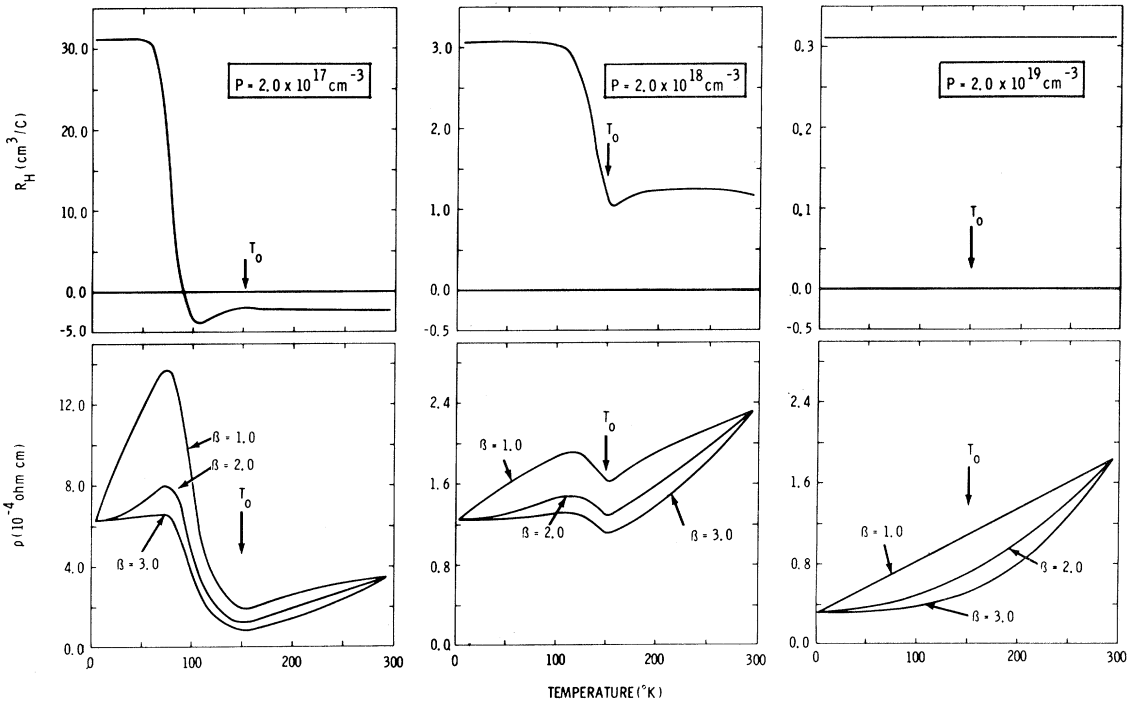


FIG. 2. Calculated temperature dependences of the Hall coefficient and resistivity of $Pb_{0.77}Sn_{0.23}Se$. The calculations were based upon the constant-mass band-inversion model described in the text.

In calculating $\rho$, it was assumed that the electron mobility $\mu_n$ is given by

$$1/\mu_n = (1/\mu_R) + CT^{\beta}. \tag{7}$$

In this relation $\mu_R$ is the low-temperature residual mobility and $C$ and $\beta$ are constants. This relation was selected as a basis for the calculations because it provides a reasonably good description of our experimental results. The calculated values of $\mu_n$ and $\mu_p$ were used along with the corresponding calculated values of $n$ and $p$ to determine $\rho$ by applying the standard two-carrier equation

$$\rho = (ne\mu_n + pe\mu_p)^{-1}. \tag{8}$$

The results of our calculations are presented in Fig. 2. They apply to $p$-type materials with three different extrinsic-carrier concentrations, selected so as to demonstrate the evolution of various features of the curves. In agreement with expectations, the results indicate large intrinsiclike variations in both $R_H$ and $\rho$ at relatively low temperatures. The variations are largest for the lowest extrinsic-carrier concentrations, becoming progressively less significant as the carrier concentration increases.

The variations in $R_H$ calculated for an extrinsic-carrier concentration of $2\times10^{17}$ cm$^{-3}$ are of particular interest. For this case, $R_H$ decreases rapidly from about 80 to 100 °K. At higher temperatures $R_H$ becomes negative, partially due to the fact that the mobility ratio $b$ is greater than 1. Such behavior is typical of that found in many other semiconductors when contributions from thermally excited carriers become increasingly important. We wish to point out, however, that the relatively constant value of $R_H$ after it has become negative is unusual. Normally, intrinsic behavior involves a strong temperature dependence of $R_H$ in this temperature region. An analysis based upon our model indicates that the unexpected constancy of $R_H$ is the result of a balance between two opposing mechanisms. The first of these is the increasing thermal energy which increases the number of carriers as the temperature rises. The second is the increasing energy gap which reduces the number of thermally excited carriers as the temperature is increased. The high degree to which these two mechanisms balance one another will be illustrated in Sec. V by calculations based upon our experimental results.

The resistivity calculations were carried out for three different values of $\beta$, the parameter representing the power of $T$ in Eq. (7). The powers 1–3 were selected because they cover the range which affords a reasonably good description of our experimental data. In carrying out the calculations, the quantities $\mu_R$ and $C$ in Eq. (7) were adjusted so as to give values of $\rho$ at 4.2 and 300 °K which are typical of those observed in these materials. A potentially useful characteristic of the

resistivity curves applying to low carrier concentrations is the distinct minimum which occurs very near the temperature $T_0$. This characteristic is of considerable interest because it suggests an experimental means of determining the temperature at which band inversion takes place.

## V. EXPERIMENTAL RESULTS

### A. $p$-Type Material

Experimental results for sample A, with an extrinsic concentration of $2.3\times10^{17}$ cm$^{-3}$, are presented in Fig. 3. Both $R_H$ and $\rho$ vary strongly with temperature in the manner given by the calculated curves of Fig. 2 for a hole concentration of $2\times10^{17}$ cm$^{-3}$.

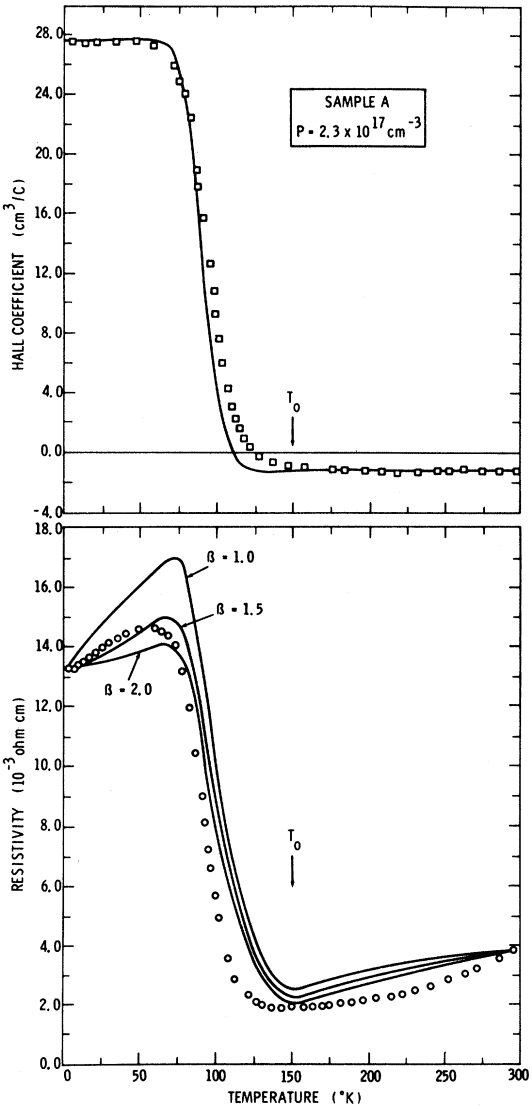


FIG. 3. Observed electrical properties of $p$-type $Pb_{0.77}Sn_{0.23}Se$ having a extrinsic-hole concentration of $2.3\times10^{17}$ cm$^{-3}$. The various curves represent calculations based upon our constant-mass band-inversion model, as discussed in the text.

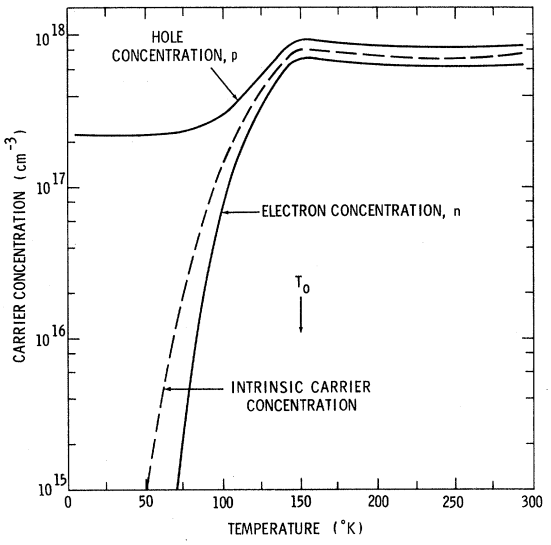


FIG. 4. Calculated temperature dependence of the electron and hole concentrations corresponding to the observed variations of $R_H$ and $\rho$ for sample A presented in Fig. 3. The broken curve represents the intrinsic-carrier concentration.

The solid curves in Fig. 3 represent values for $R_H$ and $\rho$ calculated for the specific extrinsic-carrier concentration of sample A. In doing this, we have employed the simple model described in Sec. IV. The parameters of Eqs. (6) and (7) were adjusted to obtain the best fit to the experimental data. The values adopted for these parameters are listed in Table II. The values $m^*$ and $\mu_n/\mu_p$ which are listed there, were determined by the curve-fitting process to within ±40 and ±20%, respectively. It can be seen that there is good agreement between calculation and experiment, thus confirming the appropriateness of our simple model. More importantly, however, the agreement serves as strong support for the general validity of the band-inversion model as applied to this alloy, since we know of no other band model which would yield results consistent with our observations.

The calculated values of $n$ and $p$ for sample A are represented in Fig. 4 as the solid curves. At low temperatures, $p$ is equal to the extrinsic value of $2.3\times10^{17}$ cm$^{-3}$ and is temperature independent. The values of $n$ in this region are negligible. Both $n$ and $p$ increase rapidly with temperature near 75 °K because of thermal excitation of carriers. These rapid variations continue up to near the temperature $T_0$, above which $n$ and $p$ become nearly equal to each other and are relatively temperature independent. The abrupt change in the temperature dependence which occurs near $T_0$ is a direct consequence

of the discontinuity in the temperature coefficient of $E_{gap}$ which occurs there. It is this abrupt change in the temperature dependence of $n$ and $p$ which produces the minimum in the resistivity curve which is observed near $T_0$. The nearly constant values of $n$ and $p$ at temperatures above $T_0$ are the result of a balance between two opposing mechanisms, as discussed in Sec. IV. It is this constancy which leads to the relatively temperature-independent $R_H$ which is observed in this temperature region. The broken curve in Fig. 4 represents the intrinsic-carrier concentration calculated for sample A. It is the limiting carrier concentration which one could hope to achieve by reducing the extrinsic-carrier concentration.

Experimental results for sample B having an extrinsic-hole concentration of $2.1\times10^{20}$ cm$^{-3}$ are presented in Fig. 5. The observed temperature dependences of $R_H$ and $\rho$ are characteristic of a degenerate semiconductor, despite the fact that band inversion is presumably taking place. The large unusual variations described above for sample A have disappeared. Such simplification is to be expected on the basis of our simple band-inversion model. This assertion is supported by calculations based upon the model and the parameters listed in Table II. The results are presented as the solid curves in Fig. 5, and they are in good general agreement with our observations. There is no strong evidence for the complicating phenomena discussed previously. However, it is possible that such phenomena play a role in producing the slowly increasing values of $R_H$ with increasing temperature which are observed but which are not described by our model. Such dependences are typical of degenerate semiconductors of this general type.[17] In several such cases, the behavior has been attributed to either multiple bands[21-23] or changing statistics.[23,24] In addition, the work of Allgaier suggests that band distortions

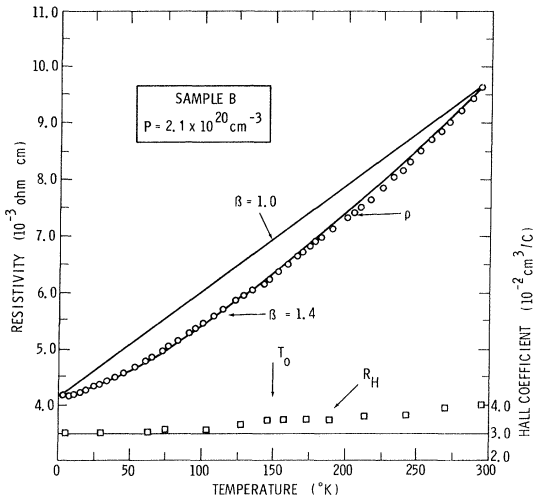


FIG. 5. Observed electrical properties of $p$-type $Pb_{0.77}Sn_{0.23}Se$ having an extrinsic-hole concentration of $2.1\times10^{20}$ cm$^{-3}$. The various curves represent calculations based upon our constant-mass band-inversion model, as discussed in the text.

may play a significant role.[25] Unfortunately, we have not been able to establish the origin of the behavior in $Pb_{0.77}Sn_{0.23}Se$.

### B. $n$-Type Material

Our experimental results for sample C with an extrinsic-electron concentration of $1.1\times10^{18}$ cm$^{-3}$ are presented in Fig. 6. The solid curves for $R_H$ and $\rho$ represent values calculated on the basis of our model and the parameters listed in Table II. A comparison of the calculated curves with the experimental results indicates that the model does not provide an adequate description of the observed results. For the Hall coefficient, the model predicts a sharp drop off near 100 °K followed by relatively

TABLE II. Electrical parameters of Eqs. (5)–(8) used for calculating the Hall-coefficient and resistivity curves presented in Figs. 3, 5, 6, and 7.

| Sample | Type | $N$[a] (cm$^{-3}$) | $m^*/m_e$[b] | $\mu_n/\mu_p$[b] | $\mu_R$[c,d] (cm$^2$/V sec) | $\mu_{300}$[c,e] (cm$^2$/V sec) | $\beta$ |
|---|---|---|---|---|---|---|---|
| A | $p$ | $2.3\times10^{17}$ | 0.1 | 1.5 | 2060 | 930 | 1.0, 1.5, 2.0 |
| B | $p$ | $2.1\times10^{20}$ | (0.1) | (1.5) | 72 | 50 | 1.0, 1.4 |
| C | $n$ | $1.1\times10^{18}$ | (0.1) | (1.5) | 27500 | 1170 | 1.5, 2.0, 2.5 |
| D | $n$ | $1.7\times10^{19}$ | (0.1) | (1.5) | 2620 | 500 | 1.0, 1.5, 2.0 |

[a] $N$ is taken to be the experimentally determined carrier concentration at 4.2 °K listed in Table I.

[b] These parameters were determined by curve fitting the experimental data of sample A. The parentheses indicate that the values for sample A were assumed to be appropriate. In the later cases, curve fitting did not yield more reliable values.

[c] These are the majority carrier mobilities.

[d] $\mu_R$ approximates the experimentally determined mobility at 4.2 °K.

[e] $\mu_{300}$ is the mobility at 300 °K as calculated from Eq. (7). Consequently, $\mu_{300}$ serves to define the constant $C$ in that equation.

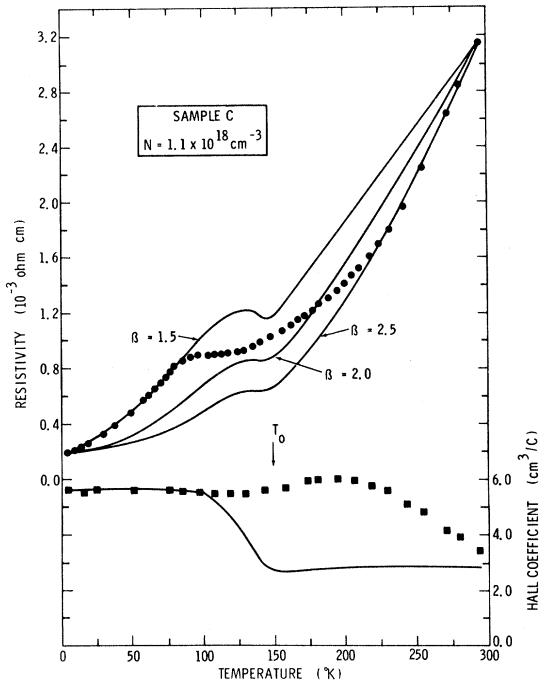


FIG. 6. Observed electrical properties of $n$-type $Pb_{0.77}Sn_{0.23}Se$ having an extrinsic-electron concentration of $1.1\times10^{18}$ cm$^{-3}$. The various curves represent calculations based upon our constant-mass band-inversion model, as discussed in the text.

temperature-independent behavior at higher temperatures. This is in contrast to the experimental data, which have a shallow minimum near 130 °K, a maximum around 200 °K, and a pronounced decrease in $R_H$ as the temperature is increased. For the resistivity, the calculated curves display distinct dips near $T_0$. According to the model, these dips are associated with the changes in carrier concentration which are evidenced by the sharp drop off in the calculated Hall coefficient. In contrast, the observed resistivity shows a break in its temperature dependence near 80 °K where the observed Hall coefficient gives no indication of a corresponding variation in the carrier concentration. These differences represent major discrepancies between the model and our observations.

We believe that the discrepancies are the result of one or more of the complicating mechanisms mentioned in Sec. III. We have explored several such possibilities including multiple-band effects, band distortions, and semimetallic behavior. Although more experimental information will be required to definitely identify the mechanisms involved, our analysis suggests that effective-mass variations play an important role, as discussed in Sec. VI.

Despite the discrepancies described above, the resistivities in the low- and high-temperature regions are well described by the calculated curves corresponding to $\beta$'s of 1.5 and 2.5, respectively. This represents a change in the power of $T$ in Eq. (7) for the carrier mobility. Such a variation is not unusual for materials of this type.[17] These agreements should not, however, be considered as significant support for the band-inversion model, because it can be shown that other band models could lead to similar results.

The experimental results for sample D having an extrinsic-electron concentration of $1.7\times10^{19}$ cm$^{-3}$ are presented in Fig. 7. As in the case of sample B, the data are typical of a degenerate semiconductor. There is no evidence of unusual variations in the temperature dependence of either $R_H$ or $\rho$ which are attributable to band inversion. These findings are consistent with the results expected on the basis of our model, as illustrated by the calculated curves based upon the parameters given in Table II. It should be noted that the resistivity data at low and high temperatures are best described, respectively, by the calculated curves for $\beta = 1.5$ and 2.0. This suggests that the temperature dependence of the carrier mobility changes as the temperature is varied. As mentioned previously, such a change is not unexpected. The slow increase in the experimental values of $R_H$ with increasing temperature is similar to that observed for $p$-type sample B. As discussed for the latter case, this variation could be due to multiple bands, changing statistics,

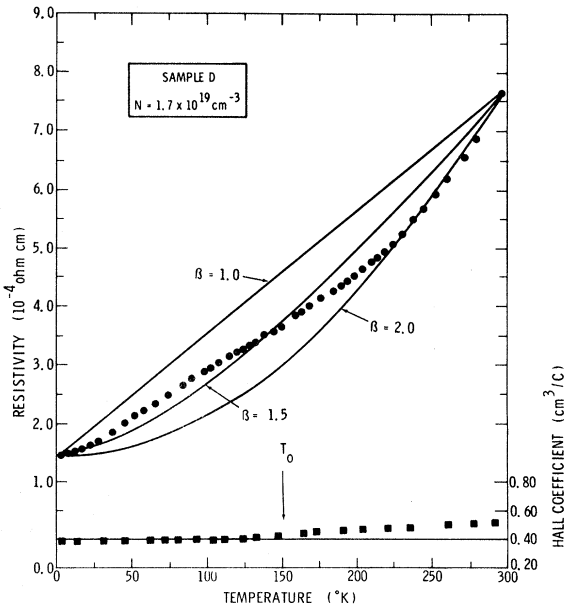


FIG. 7. Observed electrical properties of $n$-type $Pb_{0.77}Sn_{0.23}Se$ having an extrinsic-electron concentration of $1.7\times10^{19}$ cm$^{-3}$. The various curves represent calculations based upon our constant-mass band-inversion model, as discussed in the text.

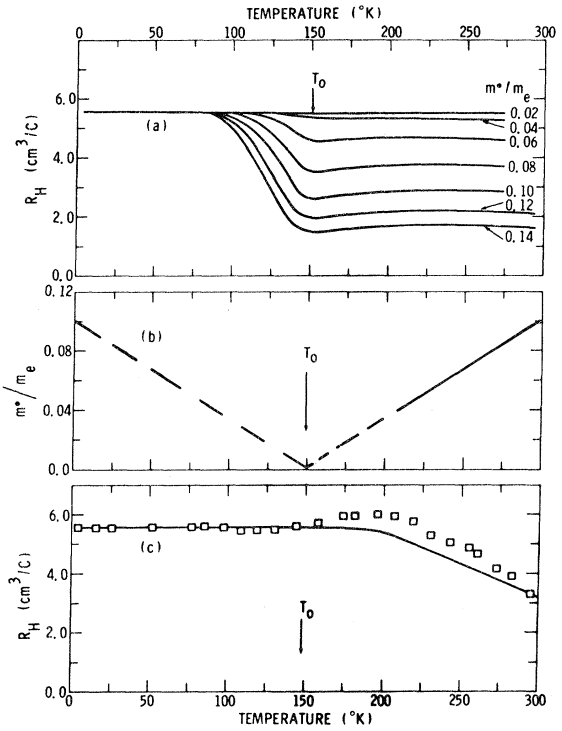


FIG. 8. (a) Calculated temperature dependence of the Hall coefficient for sample C based upon our constant-mass band-inversion model as applied to various carrier effective masses. (b) An assumed variation of the carrier effective mass resulting from the temperature dependence of $E_{gap}$ for the alloy $Pb_{0.77}Sn_{0.23}Se$. The significances of the broken and solid portions of the curve are discussed in the text. (c) Calculated temperature dependence of $R_H$ for sample C based upon the relations given in parts (a) and (b) of this figure. This dependence is represented by the curve and is to be compared with the observed values given by the data points.

or band distortions. However, the fact that similar variations are observed for both $p$- and $n$-type materials suggests that multiple bands do not play a major role.

## VI. EVIDENCE FOR EFFECTIVE-MASS VARIATIONS

As discussed in Sec. V B, discrepancies exist between the observed temperature dependences of $R_H$ and $\rho$ for sample C and the dependences calculated on the basis of our model of band inversion. We believe that effective-mass variations play a major role in producing these discrepancies.

One would expect that effective-mass variations would be associated with band inversion since small and widely varying energy gaps are involved. We have carried out an elementary analysis to determine the influence of such mass variations upon the temperature dependence of $R_H$ for sample C. The results are presented in Fig. 8. The curves in the upper section represent values of $R_H$ calculated on the basis of our model for various fixed values of the effective mass. Below about 80 °K, $R_H$ is independent of the mass, but at higher temperatures it becomes sensitive to changes in the mass. We believe that this unusual sensitivity plays an important role in determining the observed temperature dependence of $R_H$ for a material like sample C. To illustrate this point we have calculated the temperature dependence of $R_H$ corresponding to the relations of Fig. 8(a) and the effective-mass variations shown in Fig. 8(b). The latter relation was obtained by (i) matching the calculated to the experimental values of $R_H$ at 300 °K, (ii) assuming that $m^*$ is proportional to $E_{gap}$, and (iii) employing the temperature dependence of $E_{gap}$ given in Fig. 1. The results of the calculations are presented in Fig. 8(c) and they show the same gradual decrease in $R_H$ above about 200 °K which we have observed for sample C. Thus, most of the discrepancy between the calculated and experimental $R_H$ illustrated in Fig. 6 is removed by a temperature-dependent effective mass.

We wish to emphasize that the good agreement between the features of our observations and those of our calculations does not serve as an over-all validation of the mass-temperature relationship presented in Fig. 8(b). In particular, the parts of the relationship represented by the broken curve are not at all well established by our analysis. On the other hand, we believe that the solid portion of the curve is valid enough to serve as reliable evidence that effective-mass variations are taking place in this material.

Another limitation pertaining to Fig. 8(b) is that the assumed temperature dependence of $m^*$ is probably unrealistic because it is symmetrical about $T_0$. Recent experimental work by Calawa *et al.*[5] indicates that effective masses before and after inversion are different for a given $E_{gap}$. They attribute this to differing interactions with higher-level bands. Unfortunately, our results do not serve as a useful test of this expected asymmetry because $R_H$ is insensitive to the mass in the low-temperature region, as discussed above.

Finally, the effective mass at liquid-helium temperature given in Fig. 8(b) is larger by about a factor of 2 than the value which we estimate from the band-edge measurements on $Pb_{0.78}Sn_{0.22}Se$ reported by Calawa *et al.*[5] We believe that this difference is explainable in terms of the strong nonparabolicity which characterizes the bands and the uncertainty of our value of $m^*$.

Mass-variation analyses of the type described above have been carried out also for samples A, B, and D. These analyses show that the influence of effective-mass variations upon $R_H$ for such materials should be relatively small. Specifically, our calculations indicate that none of the general fea-

tures of the Hall-coefficient curves presented in Figs. 3, 5, and 7 would be altered significantly by mass variations of the type depicted in Fig. 8(b).

It is likely that effective-mass variations of the type described above are also involved in producing the discrepanies between the calculated and observed resistivities of sample C. We have not been able to carry out a meaningful quantitative analysis of this relationship because the carrier scattering mechanisms involved are not well enough known. However, it follows directly from simple qualitative reasoning that the decrease in the observed temperature coefficient of $\rho$ near 80 °K can be attributed to effective-mass variations of type discussed above. This reasoning is based upon the fact that the carrier mobility tends to increase as the carrier mass decreases. Thus, the decrease in mass as the temperature increases to $T_0$ can be expected to compensate for the normal tendency of the mobility to decrease due to increased lattice scattering. This could lead to a decrease in the temperature coefficient of $\rho$, in agreement with observation.

## VII. SUMMARY

The electrical properties of $Pb_{0.77}Sn_{0.23}Se$ are influenced by valence-conduction-band inversion. The effect is especially pronounced for low carrier concentrations, but becomes small in the high-carrier-concentration range. In addition, the experimental results suggest that the carrier effective mass changes considerably as a result of the varying energy gaps involved in the inversion process. There is no strong evidence of the multiple-band effects which characterize other materials of this general type.

## ACKNOWLEDGMENTS

We would like to thank Dr. R. S. Allgaier, Dr. R. F. Bis, and Dr. B. B. Houston of the Naval Ordinance Laboratory for many helpful discussions during the course of this work.

---

†Work partially supported by the U. S. Navy Air Systems Command under Task No. A-310-310B/WR 008-03-02.

*Research constitutes a portion of a thesis submitted to the University of Maryland by G. F. Hoff in partial fulfillment of the requirements for the Ph. D. degree in physics.

[1]A. J. Strauss, Phys. Rev. 157, 608 (1967).

[2]J. O. Dimmock, I. Melngailis, and A. J. Strauss, Phys. Rev. Letters 16, 1193 (1966).

[3]J. F. Butler, A. R. Calawa, and T. C. Harman, Appl. Phys. Letters 9, 427 (1966).

[4]T. C. Harman, A. R. Calawa, I. Melngailis, and J. O. Dimmock, Appl. Phys. Letters 14, 333 (1969).

[5]A. R. Calawa, J. O. Dimmock, T. C. Harman, and I. Melngailis, Phys. Rev. Letters 23, 7 (1969).

[6]P. A. Wolff, Phys. Rev. Letters 24, 266 (1970).

[7]I. Melngailis and T. C. Harman, in *Semiconductors and Semimetals*, Vol. 5, edited by R. K. Willardson and A. C. Beer (Academic, New York, 1970), p. 111.

[8]A. R. Calawa, T. C. Harman, M. Finn, and P. Youtz, Trans. AIME 242, 374 (1968).

[9]A. J. Strauss, Trans. AIME 242, 354 (1968).

[10]G. F. Hoff and J. R. Dixon, Bull. Am. Phys. Soc. 13, 1378 (1968).

[11]R. F. Bis, J. R. Dixon, and G. F. Hoff, Bull. Am. Phys. Soc. 12, 889 (1967).

[12]J. R. Dixon and R. F. Bis, Phys. Rev. 176, 1942 (1968).

[13]J. R. Dixon and G. F. Hoff, Solid State Commun. 7, 1777 (1969).

[14]J. C. Woolley and Orazio Berolo, Mat. Res. Bull. 3, 445 (1968).

[15]A. J. Strauss and R. F. Brebick, J. Phys. (France) 29, Suppls. 11, 12, C4-21 (1968).

[16]Other semiconductors which have this small-gap feature are gray Sn, HgTe, and $Hg_{1-x}Cd_xTe$.

[17]Yu. L. Ravich, B. A. Efimova, and I. A. Smirnov, *Semiconducting Lead Chalcogenides* (Plenum, New York, 1970).

[18]N. S. Baryshev, A. S. Makarov, K. Ya. Shtevel'man, and I. S. Aver'yanov, Fiz. Tekh. Poluprov. 2, 1024 (1968) [Sov. Phys. Semicond. 2, 852 (1969)].

[19]J. S. Blakemore, *Semiconductor Statistics* (Mac Millan, New York, 1962), p. 75.

[20]R. Dalven, *Infrared Physics*, Vol. 9 (Pergamon, London, 1969), p. 141.

[21]R. S. Allgaier and B. B. Houston, Jr., in *Proceedings of the International Conference on the Physics of Semiconductors, Exeter, England*, 1962 (The Physical Society, London, 1962), p. 172.

[22]R. S. Allgaier and B. B. Houston, Jr., J. Appl. Phys. 37, 302 (1966).

[23]T. O. Farinre, Ph. D. dissertation (University of Pennsylvania, Philadelphia, Pa., 1970) (unpublished).

[24]R. S. Allgaier and W. W. Scanlon, Phys. Rev. 111, 1029 (1958).

[25]R. S. Allgaier, Phys. Rev. 152, 808 (1966).